

# BIMCV COVID-19+: a large annotated dataset of RX and CT images from COVID-19 patients

Maria de la Iglesia Vayá<sup>1\*</sup>, Jose Manuel Saborit<sup>1</sup>,  
Joaquim Angel Montell<sup>1</sup>, Antonio Pertusa<sup>2\*</sup>, Aurelia Bustos<sup>3\*</sup>,  
Miguel Cazorla<sup>2</sup>, Joaquin Galant<sup>4</sup>, Xavier Barber<sup>5</sup>,  
Domingo Orozco-Beltrán<sup>5\*</sup>, Francisco Garcia<sup>1,7</sup>, Marisa Caparrós<sup>1</sup>,  
Germán González<sup>2,6\*</sup>, Jose María Salinas<sup>1,4\*</sup>

April 6, 2024

1. Unidad Mixta de Imagen Biomédica FISABIO-CIPF. Fundación para el Fomento de la Investigación Sanitario y Biomédica de la Comunidad Valenciana. Valencia, Spain. 2. Universidad de Alicante, Spain. 3. Medbravo. 4. Hospital San Juan de Alicante, Spain. 5. Universidad Miguel Hernández, Spain. 6. Sierra Research SL. 7. Bioinformatics & Biostatistics Unit, CIPF. Valencia, Spain. \*corresponding authors: Maria de la Iglesia Vayá (de-laiglesia\_mar@gva.es), Antonio Pertusa (pertusa@ua.es), Aurelia Bustos (aurelia@medbravo.org), Domingo Orozco-Beltrán (dorozco@umh.es), Germán González (ggonzalez@sierra-research.com), Jose Maria Salinas (salinas\_josser@gva.es)

## Abstract

In this work we describe BIMCV-COVID-19+ dataset, a large dataset from Medical Imaging Databank in Valencian Region Medical ImageBank (BIMCV) with chest X-ray images CXR (CR, DX) and computed tomography (CT) imaging of COVID-19+ patients along with their radiological findings and locations, pathologies, radiological reports (in Spanish), DICOM metadata, Polymerase chain reaction (PCR), Immunoglobulin G (IgG) and Immunoglobulin M (IgM) diagnostic antibody tests. The findings are mapped onto standard Unified Medical Language System (UMLS) terminology and they cover a wide spectrum of thoracic entities, contrasting with the much more reduced number of entities annotated in previous datasets. Images are stored in high resolution and entities are localized with anatomical labels in a Medical Imaging Data Structure (MIDS) format. In addition, 10 images were annotated by a team of radiologists to include semantic segmentation of radiological findings. This first iteration of the database includes 1,380 CX, 885 DX and 163 CT studies from 1,311 COVID-19+ patients. To the best of our knowledge, this is the largest COVID-19+ dataset of images available in an open format. The dataset can be downloaded from <http://bimcv.cipf.es/bimcv-projects/bimcv-covid19/>.


	<p><b>Report:</b> opacidades de aspecto intersticioalveolar parcheadas y bilaterales que predominan en ambos lobulillos inferiores sospechosas de infección por COVID-19 . senos costofrenicos libres .</p> <p><b>Labels:</b> COVID 19, alveolar pattern, interstitial pattern, pneumonia</p> <p><b>Locations:</b> costophrenic angle, lobar, bilateral, lower lobe</p>																												
<table><tr><th>DICOM Fields</th></tr><tr><td>Study Date 20200317</td></tr><tr><td>Patient's Sex M</td></tr><tr><td>Patient's Birth Date 1986</td></tr><tr><td>Modality CR</td></tr><tr><td>Manufacturer GE Healthcare</td></tr><tr><td>...</td></tr></table>	DICOM Fields	Study Date 20200317	Patient's Sex M	Patient's Birth Date 1986	Modality CR	Manufacturer GE Healthcare	...	<table><tr><th>Date</th><th>Test</th><th>Result</th></tr><tr><td>17.03.2020</td><td>PCR</td><td>NEGATIVE</td></tr><tr><td>18.03.2020</td><td>PCR</td><td>NEGATIVE</td></tr><tr><td>19.03.2020</td><td>IGG</td><td>POSITIVE</td></tr><tr><td>19.03.2020</td><td>IGM</td><td>POSITIVE</td></tr><tr><td>20.03.2020</td><td>PCR</td><td>POSITIVE</td></tr><tr><td>...</td><td>...</td><td>...</td></tr></table>	Date	Test	Result	17.03.2020	PCR	NEGATIVE	18.03.2020	PCR	NEGATIVE	19.03.2020	IGG	POSITIVE	19.03.2020	IGM	POSITIVE	20.03.2020	PCR	POSITIVE	...	...	...
DICOM Fields																													
Study Date 20200317																													
Patient's Sex M																													
Patient's Birth Date 1986																													
Modality CR																													
Manufacturer GE Healthcare																													
...																													
Date	Test	Result																											
17.03.2020	PCR	NEGATIVE																											
18.03.2020	PCR	NEGATIVE																											
19.03.2020	IGG	POSITIVE																											
19.03.2020	IGM	POSITIVE																											
20.03.2020	PCR	POSITIVE																											
...	...	...																											

Table 1: Example of an image on the dataset and its associated information. Top left: image with the ROIs for ground glass opacities (green) and consolidations (purple) as marked by a trained radiologist. Top right: radiology report (in Spanish), radiological findings, differential diagnosis and locations as extracted using natural language processing from the radiology report. Bottom left: example of the image metadata as obtained from the DICOM fields. Bottom right: diagnostic tests performed to this subject, showing positive results for IGG and IGM on 19/03/2020 and positive in PCR on 20/03/2020.

## Background & Summary

SARS-Cov-2 has created an unprecedented pandemic situation. The scientific community has focused on the development of artificial intelligence (AI) algorithms for the better diagnosis and prognosis of COVID-19+ patients. However, such efforts are often performed on proprietary datasets, whereas few image studies of patients positive for COVID-19 are publicly available.

During the first half of March 2020, the American College of Radiology (ACR) published guidelines concerning medical imaging for COVID-19 diagnosis [1]. Among some of its recommendations, they include that “CT should not be used to screen for or as a first-line test to diagnose COVID-19, CT should be used sparingly and reserved for hospitalized, symptomatic patients with specific clinical indications for CT”. This recommendation is in line with our initial commitment to focus on conventional radiology as a tool to aid diagnosis, prognosis and triage of COVID-19 patients.

The BIMCV COVID-19+ dataset is a large and open multi-institutional data-bank to provide the open scientific community with data of clinical-scientific value that helps early detection and evolution of COVID-19. Given the current COVID-19 pandemic, both speed and efficiency in developing accurate medical solutions are key factors so that they can reach the clinical environment in the shortest possible time. Making the information accessible to the scientific community worldwide will undoubtedly maximize the usefulness of the data.

Some well-known examples of the scope and benefit of open access medical datasets are:

- Pan-cancer Atlas (TCGA) [2] of the National Cancer Institute, whose open exploitation has been essential for the development of new treatments in precision medicine in cancer.
- MIMIC dataset [3, 4]: MIMIC-III is a widely used and freely accessible data set developed by the MIT Laboratory for Computational Physiology, comprising de-identified health data associated with more than 40,000 critical care patients.
- Padchest [5] from Valencian Region Medical Image Bank (BIMCV) is one of the largest chest radiography image data banks (hereinafter CRX), amounting to 166,000 images tagged with all observable medical entities along with their anatomical locations.

This dataset is intended to be incremental, therefore new images along with their annotations will be continuously added when available. At this time (first iteration), BIMCV COVID-19+ contains 1,380 CR, 885 DX, and 163 CT full-resolution images from 1,311 patients.

The data provided for each study, detailed in Sec. Data Records, include the images, anonymized DICOM metadata, anonymized radiologic reports (in Spanish), and UMLS biomedical vocabulary unique identifiers (CUIs) associated to each image (for example, ‘infiltrate’, ‘pleural effusion’, etc.) organized in

semantic trees. In addition, 10 images were manually annotated by a team of radiologists with the Regions of Interest (ROI) of the findings that are related to COVID-19.

Regarding previous COVID-19 datasets, Table 2 summarizes the main features of the datasets published so far. First, we describe the public datasets.

Table 2: Main characteristics of the different datasets with COVID-19 information published so far. The highlighted features are: #Imag. number of COVID-19 images; #Pat. number of patients; Sex; Age; Diagnostics: COVID, No (COVID), Others (pneumonia caused from other virus); Surv. information about the patient survival; View: Patient position; #Rx: number of Rx images; #CT: number of CT images; Rad.Rep.: Radiological Reports; Pub.: Public.

Dataset	#Imag.	#Pat.	Sex	Age	Diagnostics
COVID-CHESTXRAY [6]	373	205	✓	✓	COVID/Others
COVID-CT [7]	349	216	✓	✓	COVID/No
SIRM-COVID [8]	340	85	✓	✓	COVID
COVID-19 RAD. DB. [9]	219	Unknown	✗	✗	COVID/No/Others
Private dataset [10]	1,296	Unknown	✗	✗	COVID/No/Others
Private dataset [11]	877	Unknown	✗	✗	COVID/No
Private dataset [12]	1,658	Unknown	✗	✗	COVID/No/Others
<b>BIMCV COVID-19+</b>	<b>5,381</b>	<b>1,311</b>	✓	✓	COVID/No/Others

Dataset	Surv.	View	Rx	CT	Rad.Rep.	Pub.
COVID-CHESTXRAY [6]	✓	✓	10	10	✓	✓
COVID-CT [7]	✗	✗	✗	349	✓	✓
SIRM-COVID [8]	✗	✓	255	85	✓	✓
COVID-19 RAD. DB. [9]	✗	✗	219	✗	✗	✓
Private dataset [10]	✗	✗	✗	1296	✗	✗
Private dataset [11]	✗	✗	✗	877	✗	✗
Private dataset [12]	✗	✗	✗	1658	✗	✗
<b>BIMCV COVID-19+</b>	✗	✓	<b>3,141</b>	<b>2,239</b>	✓	✓

COVID-CHESTXRAY [6] is a public dataset of pneumonia cases with chest X-ray or CT images, specifically COVID-19 cases as well as MERS, SARS, and ARDS. Data are collected from public sources in order not to infringe patient confidentiality, and contains data from 205 patients. COVID-CT [7] is a CT public dataset. Images are collected from COVID-19 related publications, extracting them directly from papers in PDF format. Therefore, the quality of images is not optimal. The number of patients is similar to the previous one. SIRM-COVID [8] is a dataset of COVID-19 cases with RX and CT images. It only contains positive cases, and it includes both radiological and clinical reports. COVID-19 RADIOGRAPHY DATABASE [9] is published in Kaggle and contains a large number of normal Rx (1,341) and other viral pneumonia images (1,345). However, it contains few COVID-19 positive images.

There are also some private datasets. In [10], authors describe a non-public dataset that contains a large number of CT images along with 1,735 samples

for community acquired pneumonia and 1,325 for non-pneumonia. Another private CT dataset is described in [11]. In this case, it contains 877 COVID-19+ images and 541 COVID-. Finally, [12] also has a private CT dataset, with 1,659 positives and 1,027 with community acquired pneumonia.

In summary, to the best of our knowledge, BIMCV COVID-19+ is the first dataset that includes radiological findings. In addition, it is the only COVID-19 bank in which some images are labeled with Regions of Interest (ROI) annotated by radiologists. Moreover, it is the largest dataset in number of images and patients, and it includes multiple samples for each patient to analyze their clinical evolution. The dataset is intended to be incremental and it will grow when as soon as images will be available. This work describes the dataset at its first iteration (version 1), with release date 28/05/2020.

## Methods

This section addresses the methodology used to produce the data. We also describe the ethics involved the process of data acquisition, the data anonymization, and the labeling process.

### Ethics statement

The Institutional Review Board (IRB) of the Miguel Hernandez University (MHU) approved this HIPAA-compliant retrospective cohort study. The study was approved by the local institutional ethics committee CELm: 12/2020 in Arnau de Vilanova Hospital in Valencia Region. The healthcare authorities of the Comunitat Valenciana authorized the publication of the open database based on different reports that had to be written, among them the following should be highlighted: A favorable report from the Data Protection Officer (DPO). A development report of a Impact study. PIs confidentiality agreement. A confidentiality agreement between researchers. The declaration of a data protection officer for all participating entities. Compliance report of security measures proposed in the DPO report and finally a detailed risk study together with mitigation measures of detected risks.

### Data acquisition

For data acquisition, we follow the process described in [13]. R & D Cloud CEIB has four general modules: Search engine (SE), manager of clinical trials (GEBID), anonymizer (CEIBANON) and BioImage Knowledge Engine (BIKE). The technology used in R & D Cloud CEIB is completely based on Open Source.

All consecutive studies of patients with at least one positive PCR test or positive immunological tests (IgM, IgG or IgA) for SARS-Cov-2 in the period of time between February 26th and April 18th, 2020 were identified by querying the Laboratory Information System records from the Health Information Systems in Comunitat Valenciana. All medical images acquired for such subjects

in the period of time were included into the BIMCV COVID-19+ dataset. The images included chest x rays (both digital DX and digitalized film CR), as well as computed tomography scans CT. The images were retrieved from the Vendor Neutral Archive (VNA) in the central medical image repository of Digital Medical Image Management project (GIMD) that belongs to the public healthcare system in the Valencian Region (Spain). The data in its first iteration were obtained from 11 hospitals from the Valencian Region.

## Data Geo-positioning

The Valencian health system is arranged in health departments, which are equivalent to the health areas provided in the General Health Law. The health departments are the fundamental structures of the Valencian health system, being the geographical demarcations into which the territory of the Valencian Region is divided for health purposes and constituting the framework for the integration of health promotion and protection actions, prevention and cure and rehabilitation of health status; through the coordination of existing resources and guaranteeing health without steps.

In Figure 1, we show the choropleth map with the number of tests performed (CR, DX and CT) by the health departments. In this first iteration of the dataset it can be observed that most of the departments (11 concretely) are from the province of Alicante and Castellón. For future iterations it is planned to complete the map.

## Data anonymization

The Organic Law 3/2018 [14] establishes the legal framework for data protection in biomedical research. Reuse of personal data for medical research needs to be approved by an ethics committee, and data must be at least pseudonymized before the researchers get access. In this sense, anonymization is defined as “the result of the processing of personal data to irreversibly prevent its identification”. That is why anonymization in itself constitutes additional processing of personal data. Within this complex and sensitive framework, state-of-the-art anonymization techniques in Medical Imaging have been applied to BIMCV COVID-19+ dataset. The anonymization process is performed in two ways. First, all references to patient data were removed from the radiological report by using the methodology explained in [15]. This method is designed to parse Spanish reports. It uses a pre-trained Bidirectional LSTM to identify names and personal data and remove them from the report.

Second, DICOM anonymization was performed based on DICOM PS3.15 Annex E using a CTP [16] server. Finally, the images were evaluated in a semi-automatic process and some of them were visually inspected to remove or crop the burnt-in personal information from the chest x-ray images.

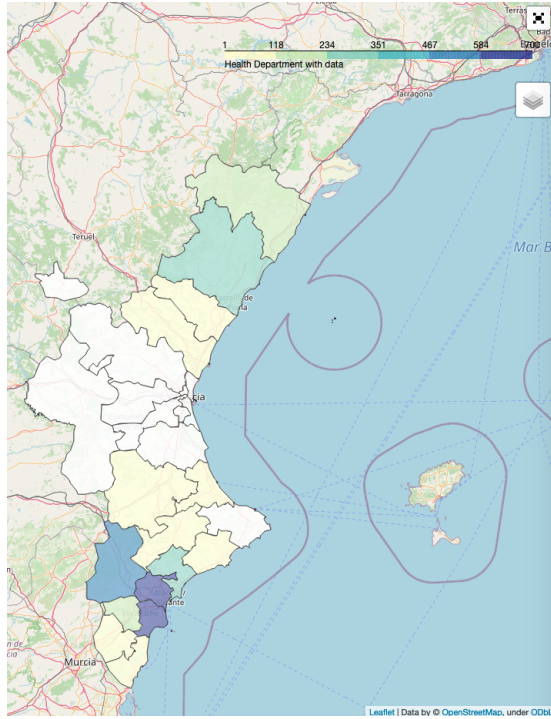


Figure 1: Choropletic map with #CR #DX #CT from first iteration. <https://maigva.github.io/maps/HealthDepartCOVID19.html>

### Radiological reports anonymization

Anonymization of radiological reports was performed by applying the DisMed methodology based on a Named Entity Recognition (NER) strategy, that is focused on the extraction and location of seven predefined entities or categories (see Table 3) belonging to radiological reports and with a set-up of this system to be adapted to the domain of medical texts.



Figure 2: Conceptual scheme of radiological report anonymization.

### DICOM anonymization

The DICOM standard has already defined the framework that guarantees safe access, exchange and processing of medical data. However, to the best of our

Table 3: Name Entities selected for anonymization and their associated Protected Health Information categories.

NEs	Description	PHIs
CAB	Section headers	
NAME	Names and surnames (patient and others)	Names
DIR	Full addresses, including streets, numbers and zip codes	Geographic data
LOC	Cities, inside and outside addresses	Geographic data
NUM	Numbers or alphanumeric strings that might identify someone, including digital signatures, patient numbers, medical numbers, medical license numbers and others	Medical record numbers, social security numbers, account numbers, any unique identifying number or code
FECHA	Dates	Dates
INST	Hospitals, health centers or other institutions	

knowledge there are no tools that implements all the confidentiality profiles defined in Part 15 of the DICOM standard [16, 17] in paragraph E 'Attribute Confidentiality Profiles', with the exception of the Clinical Trial Processor (CTP [18]). To avoid compromising data privacy, it is considered crucial to implement different modules and scripts within the CTP that will compose the development of the ten DICOM confidentiality profiles that are defined in the standard.

For each module, the scripts related to the Basic Profile have been applied, which is the strictest and that eliminates all the information related to (i) the identity as well as the identifying and demographic characteristics of the patient, (ii) the identity of the authors, responsible or relatives, (iii) the identity of any personnel involved in the procedure, (iv) the identity of the organizations involved in ordering or carrying out the method, (v) the information (not related to the patient) that could be used to find out the identity of the original anonymized files (for example, UID, date and time), and (vi) private attributes (which are not part of the standard).

The system allows different types of anonymity, from the alteration of the existing text information in DICOM headers up to image-level deformation of parts that can identify the patient (especially in neuroimaging obtained by magnetic resonance). In the case of RX/DX/CT, no image deformations were necessary since the reconstruction of the patient data is not possible from this information.

## Image preprocessing

Raw pixel data was extracted from the DICOM images and stored into files in *nii.gz* format. The images were processed by rescaling the dynamic range using the DICOM window width and center, when available and stored as 16-bit PNG



images. The images were not re-scaled to avoid resolution loss.

The information on image projection was estimated using a neural network with an EfficientNet [19] architecture. The projection estimation network was trained with 2,000 images from Padchest [5] to whom the orientation had been manually estimated. The projection was oversimplified to frontal (including antero-posterior and postero-anterior) and lateral (L). No difference was made between erect, either standing or sitting or decubitus. No difference was made between left lateral or right lateral. Such information could be inferred posteriorly by a careful analysis of the DICOM tags.

## Labeling

The early detection and location of lesions such as infiltrates, in particular ground glass opacities, is essential both for diagnosis and to predict the evolution of the patient and to help taking clinical decisions. The findings that suggest a COVID-19 infection are both the ground-glass opacity and consolidation that, even in the initial stages, affect both lungs, particularly the lower lobes, and specially the posterior segments, with a peripheral and subpleural distribution mainly [20, 21, 22, 23].

These findings were present in 44% of patients in the first two days on chest CT scans [20], in 75% of patients in the first four days [21] and in 86% of patients during illness days 0-5 [22].

These lesions can progress in the following days until they become more diffuse. If associated with septal thickening, they will have a reticular pattern. In general, they progress both in extension and towards consolidation concomitantly with the ground glass pattern, and may then present a rounded morphology. It is very rare that it associates lymphadenopathy, cavitation or pneumothorax, as did the respiratory syndrome coronavirus MERS-CoV [24].

Therefore, beyond labeling an image as COVID/No/Others like most existing datasets, it is very important to annotate the radiological findings, both for the diagnosis and for the prognosis. It should be considered that these characteristic lesions frequently appear in non-COVID patients and, on the other hand, many COVID-19 patients do not have these lesions. The appearance of the lesions is related to the level of the disease. It is characteristic that many of the patients worsen and that lesions appear or become more evident.

To the best of our knowledge, BIMCV COVID-19+ is the first COVID-19 dataset that includes these findings. In addition, in this first iteration, ten images are also annotated with the ROIs of the findings.

## Assigning CUI labels to images

Clinical reports were used as a basis to obtain the radiological finding, differential diagnosis and localization labels. Therefore, images were not used in this process.

In order to obtain the labels, the same procedure used to build PadChest [5] was carried out, but adding to the set of labels the COVID-19 (CUI C5203670)

and COVID-19 uncertain (CUI C5203671) labels, totaling to 336 different labels. After a preprocessing stage in which the words from the radiological report were stemmed and tokenized, labels were automatically extracted using a deep neural network multi-label classifier trained with the PadChest dataset. The network topology is detailed in [5], but it was re-trained with the additional COVID-19 labels.

More specifically, this classifier consists of a bidirectional LSTM with attention mechanism that receives as input a preprocessed radiographic report encoded as a sequence of pre-trained word-embeddings, and outputs the more likely labels. Labels corresponding to diagnoses, radiological findings and anatomical localizations, are mapped onto the UMLS controlled biomedical vocabulary unique identifiers (CUIs) and organized into semantic concept trees.

For example, consider the following report sentence: *Cambio pulmonar crónico severo. Signos de fibrosis bibasal. Sutil infiltrado pseudonodular milimétrico en vidrio deslustrado localizado en bases. Cifosis severa.*

In this case, the neural network would outputs the following labels: ['pulmonary fibrosis', 'chronic changes', 'kyphosis', 'pseudonodule', 'ground glass pattern'], along with their localizations when available: [['pulmonary fibrosis', 'loc basal bilateral'], ['chronic changes'], ['kyphosis'], ['pseudonodule', 'ground glass pattern', 'loc basal']].

An example PadChest semantic concept sub-tree of some lesions that are frequently associated with COVID-19 is shown next:

```

├─ infiltrates [CUI:C0277877]
│   └─ interstitial pattern [CUI:C2073538]
│       └─ ground glass pattern [CUI:C3544344]
│           └─ reticular interstitial pattern []
│               └─ reticulonodular interstitial pattern [CUI:C2073672]
│                   └─ miliary opacities [CUI:C2073583]
│   └─ alveolar pattern [CUI:C1332240]
│       └─ consolidation [CUI:C0521530]
│           └─ air bronchogram [CUI:C3669021]
│   └─ air bronchogram [CUI:C3669021]

```

As it can be seen, although the radiological reports are provided in Spanish, labels are mapped onto biomedical vocabulary unique identifier (CUIs) codes, thus making the dataset usable regardless of the language.

In addition to the PadChest labels that can be found in [5], the new “COVID-19” and “COVID-19 uncertain” labels were added as new terms, to denote high or low suspicion of COVID-19 respectively. For this end, the word-embeddings of these new labels were pre-computed in the corpus of new reports from COVID-19 patients added to the Padchest Spanish report corpus. Then, the Padchest multi-label text classifier was trained with the manually labeled reports from Padchest but adding 724 new manually annotated sentences (428 from the BIMCV COVID-19 positive partition and 296 from the BIMCV COVID-19 negative partition) referring to COVID-19 as highly likely, uncertain or negated based on the radiologist judgment, totaling up to 23,439 manually annotated

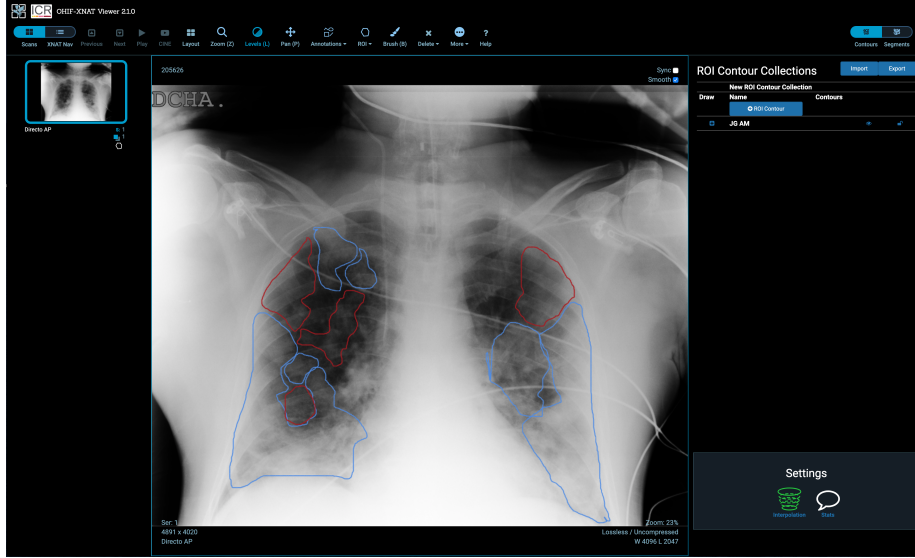


Figure 3: Example annotation at pixel level. In blue, consolidation, red marks ground glass.

sentences.

### Annotation of regions of interest

Since some lesions such as infiltrates, ground glass opacities or consolidation patterns are the most frequent in COVID-19 patients, a sub-set of 10 images were annotated with their regions of interest (ROI) by a team of eight radiologists from the Hospital Universitario de San Juan de Alicante, for the first iteration of COVID-19 dataset.

As it can be seen in Figure 3, ROIs corresponding to these findings were labeled at a pixel level using XNAT OHIF Viewer [25]. OHIF is a zero-footprint medical image viewer provided by the Open Health Imaging Foundation that stores an XML output with the ROI paths. This information is very valuable to train semantic segmentation networks such as UNet [26] in order to extract characteristics like the extension and exact location of the lesions. Table 4 shows the findings that are annotated at a ROI level.

### Code availability

The annotation pipeline from medical reports including their text preprocessing and the multi-label classifier based on bidirectional Long Short-Term Memory Networks (LSTM) with attention mechanism is available at <https://github.com/auriml/Rx-thorax-automatic-captioning>.

Id	Description
1	Ground glass XRays
2	Consolidation XRays
3	Peural effusion XRays
4	Interstitial RX
5	Ground glass CT
6	Crazy Paving CT
7	Inverted halo CT
8	Vascular thickening (in ground glass region) CT
9	Ground glass and consolidation focus CT
10	Nodular consolidation or in CT
11	Normal consolidation CT
12	Sprouting tree pattern CT
13	Pleural effusion CT
14	No RX or TAC findings

Table 4: Findings that are annotated with their ROIs using XNAT OHIF Viewer.

### Database analysis

Statistics about the dataset were acquired with a python Jupyter notebook available at <https://github.com/BIMCV-CSUSP/BIMCV-COVID-19>.

## Data Records

The BIMCV (Medical Imaging Bank of the Valencia Region) specializes in collecting and organizing data imaging information to facilitate the research in artificial intelligence and big data with medical imaging. The BIMCV team has designed MIDS (Medical Imaging Data Structure)<sup>1</sup>, a standard to organize every type of medical information and images in simple hierarchy folders. MIDS constitutes an extension of the standard BIDS (Brain Imaging Data Structure), that is a structure that collects medical resonance brain images (MRI) and is described in [27]. MIDS intends to expand BIDS, extending its usage to any type of medical imaging modality and anatomical area of the body instead of only medical brain images.

The main goal of MIDS is to define a standard for organization and description of the medical imaging datasets in the field of artificial intelligence and to facilitate data sharing. For this, we have adapted DICOM standard in an hierarchical organization that will be based on folder organization with simple file formats (TSV and JSON). The main data types for Imaging are: nifti (3D) or png (2D) files; for phenotypic data, Tab Separated Value files (.tsv); and for metadata information (Key/value dictionaries), JSON files.

<sup>1</sup><https://github.com/BIMCV-CSUSP/MIDS>

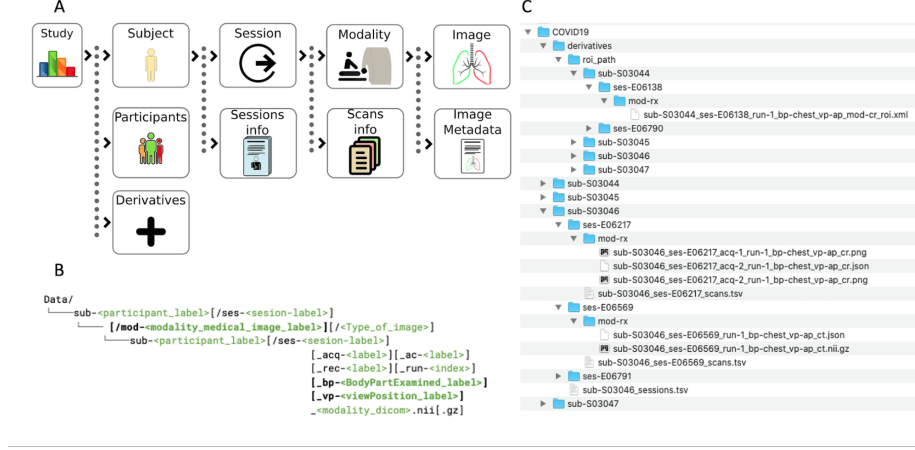


Figure 4: MIDS structure for BIMCV COVID-19+ dataset. (A) Conceptual schema (B) General Template (C) Example of folder structure.

Figure 4 shows an example from BIMCV COVID-19+ data structured in MIDS format. The data provided for each sample is described next:

**Diagnostic tests:** All the diagnostic tests performed to each individual to diagnose COVID-19. The diagnostic test could be PCR, IGG or IGM. The result of the test can be positive, negative or indeterminate. A subject can have several tests during the period of time with different outcomes. The list of tests is stored into the file *sil\_reg\_covid.csv*.

**Radiological reports:** The radiological reports for each image study performed to the subject anonymized as explained in Section Radiological reports anonymization. They are included in the file *derivatives/EHR/labels/labels\_COVID-19\_posi.tsv*.

**CUI disease and location terms:** extracted automatically using the methodology described in Subsection Labeling. They are stored in the same file than the radiological reports.

**CUI hierarchy:** a tree description of the CUI hierarchy used to describe the diseases. File *derivatives/EHR/labels/tree\_term\_CUI\_counts\_image\_covid\_posi.csv*.

**Image data:** Each subject can have a plurality of image studies, also called sessions, performed on the period of time of the observation. Each image study has a plurality of image series. They are all stored in the directory structure depicted in Fig. 4. Image data is extracted from the DICOM images and stored in *.nii.gz*. The relevant DICOM fields for each image series are stored in a JSON file with the same name than the image series.

## Technical Validation

The data collected contains 1,311 subjects, 2,429 image studies and 5,530 image series. 602 patients were female (45.92%). The mean age was of 63.11 ( $\pm 16.75$ ). The histogram of their age is shown in Fig. 5 (top) and is highly coherent with the demographics of COVID-19+ in Spain.

There is an average of 1.9 image studies per subject. The distribution can be seen in Fig. 5 (middle). With respect to image modality, the dataset contains 1,380 CX, 885 DX and 163 CT studies. 2,427 chest x-rays were acquired in monochrome 2 photometric interpretation and 751 in monochrome 1. Images in monochrome 1 should be inverted for their proper visualization. The vendors of the devices used to acquire the studies are shown on Table 5. As can be seen, there are different acquisition systems, which ensures variability in the dataset images.

Manufacturer and model	#studies
KONICA MINOLTA 0862	342
GMM ACCORD DR	255
SIEMENS SIEMENS FD-X	247
Agfa DR 14e C - 1200ms	161
Agfa DX-M	161
"GE Healthcare" "Thunder Platform"	150
Philips Medical Systems DigitalDiagnost	133
Philips Medical Systems PCR Eleva	113
Agfa 3543EZE	112
Carestream Health DRX-1	87
KONICA MINOLTA CS-7	77
SIEMENS SOMATOM go.Up	69
Agfa Pixium_4343E_CSI	59
Agfa CR30-X	39
Canon Inc. CXDI Control Software NE	37
TOSHIBA Aquilion	36
Philips DigitalDiagnost	34
KONICA MINOLTA 0110	23
Philips Brilliance 16	23
Philips Medical Systems Essenta DR	21

Table 5: Number of studies acquired by each device for devices with more than 15 studies acquired.

A total of 2,425 PCR tests have been performed on the patients, from which 1,773 resulted positive for SARS-Cov-2, 622 negative for SARS-Cov-2 and 30 indeterminate, 29 IGM 29 IGG and 35 ACT tests were performed, being 44 positive, 32 negative and 17 indeterminate. The average closest time between an image and a diagnostic test is 5.03 days, being the distribution as shown in Fig. 5 (bottom). Please note that some images have a diagnostic test as far

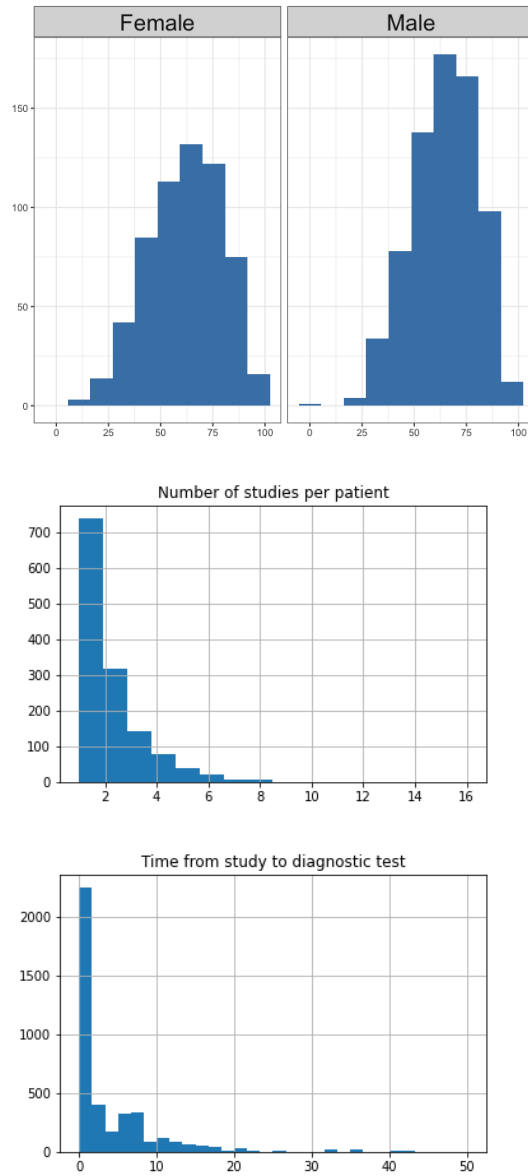


Figure 5: Top: histogram of the patients age. Middle: histogram of the number of studies per subject. Bottom: histogram of the difference (in days) between the image study and the diagnostic test. Please note that most of the studies have less than five days between the radiography and the diagnostic test.

as 50 days afterwards. Such is acceptable, since the period of observation is of

two months and there are image studies performed to the subjects prior to their COVID-19 diagnosis.

135 studies were deemed suboptimal in the radiology reports. The most common radiological findings on the images, as well as the number of their appearances, are shown in Table 6. Due to the construction of the database, COVID-19 appears as the most common radiological finding, followed by densities, pneumonia, consolidations and infiltrates, all findings closely related to COVID-19.

Image anonymization was validated by visually inspecting all the cropped images to verify that no data from the patients was displayed.

Chest x-ray images were manually inspected to validate if the patient orientation was correctly estimated with the neural network described in Section Image Preprocessing. The orientation was changed in case it was mistakenly estimated.

Radiological finding and diagnosis	Number
COVID 19	802
increased density	657
pneumonia	605
unchanged	494
consolidation	357
infiltrates	346
interstitial pattern	317
alveolar pattern	291
normal	284
ground glass pattern	240
cardiomegaly	166
pleural effusion	149
laminar atelectasis	88
costophrenic angle blunting	83
suboptimal study	82
viral pneumonia	62
endotracheal tube	59
aortic elongation	58
nodule	54
central venous catheter	54

Table 6: Radiological findings and diagnoses extracted from the radiology reports when having more than 50 appearances.

Regarding the labeling of the reports, in some of them where the text “COVID-19” was mentioned those mentions were actually negated expressions for COVID-19 disease based on image. The neural network was trained to ensure that the model could detect these COVID-19 denials and validate that the labels “COVID-19” and “COVID-19 uncertain” were correctly extracted. The model achieved an  $F1$ -micro of 0.922 on the validation set with 2,343 manually labeled



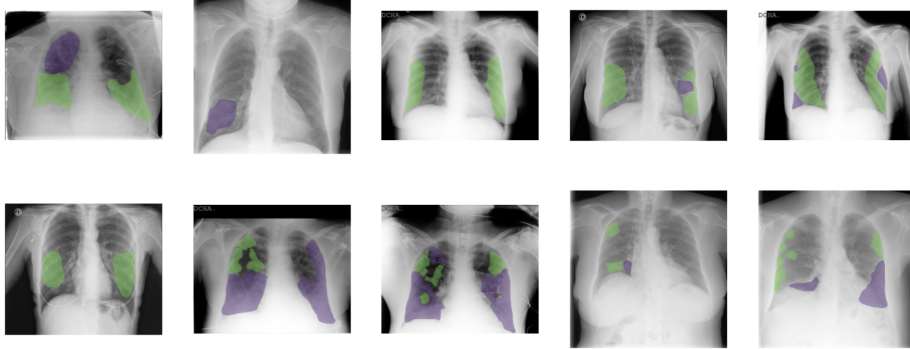


Figure 6: ROIs marked for 10 images from different series. Green: ground glass opacities. Purple: consolidations.

sentences (which includes sentences from Padchest [5], BIMCV COVID-19 positive and BIMCV COVID-19 negative partitions), and it was further validated using an independent test sample.

This independent test sample consisted of 64 new sentences manually labeled and randomly extracted from the BIMCV COVID-19 negative partition in which the text COVID-19 was mentioned. In some cases the mention was to deny it (24), in others it is to denote low suspicion based on image findings because of atypical findings “COVID 19 uncertain” (13) and in the rest (27) it was affirmatively mentioned because the image was compatible with COVID-19 even if those studies were included in the BIMCV-COVID-19 negative samples. Results on this experiment are shown in Table 7.

Radiological findings set	Precision	Recall	F-Score
COVID-19	0.961	0.925	0.943
COVID-19 uncertain	1.0	0.846	0.916

Table 7: Classification results in an independent sample test of the COVID-19 labels

In addition, the method was evaluated for all included entities, both those entities related or not related to COVID-19 pneumonia, on the same independent test set, using the metrics described in [5], obtaining an  $F1$ -weighted=0.9320,  $F1$ -micro=0.9378, and accuracy=0.8281.

## Usage Notes

This dataset offers valuable information for professionals, for example to train radiologists on this new pathology and understand the lesions that can be typically found. In addition, it serves to train deep learning methods with the images and labels in order to assist radiologists in the decision-making process.

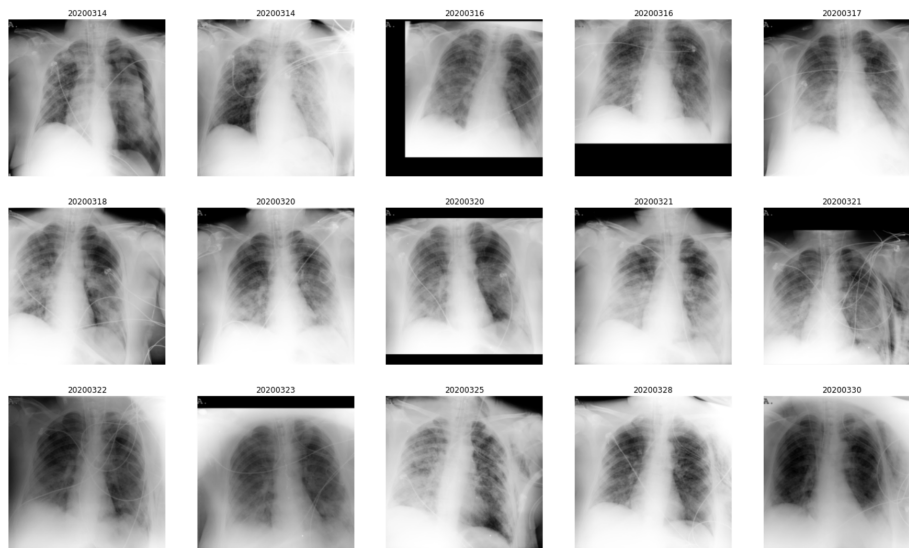


Figure 7: Longitudinal series for the same subject with 15 image studies between March 14th and March 30th 2020.

The data can be downloaded under request from the BIMCV web page (<http://bimcv.cipf.es/bimcv-projects/bimcv-covid19>). It is freely available for research, and can also be used for commercial purposes under certain conditions. Before downloading the data, the user should accept the End-User License Agreement detailed in <http://bimcv.cipf.es/bimcv-projects/bimcv-covid19/bimcv-covid19-dataset-research-use-agreement-2/>.

## Acknowledgements

This work is first and foremost an open and free contribution from authors in the working group with support from the Regional Ministry of Innovation, Universities, Science and Digital Society grant awarded through decree 51/2020 by the Valencian Innovation Agency (Spain). This research is also supported by the project UACOVID-19-18 from the University of Alicante.

Part of the infrastructure used has been cofunded by the European Union through the Operational Program of the European Fund of Regional Development (FEDER) of the Valencian Community 2014-2020 and the Medical Image Bank of the Valencian Community were partially funded by the Horizon 2020 Framework Programme of the European Union under grant agreement 688945 (Euro-BioImaging PrepPhase II).

Thanks to General Electric Healthcare, who, altruistically, has made available the technical and human means necessary to perform parameterized searches, and to the Bioinformatics and Biostatistics Unit of the CIPF, which is located

within the ‘TransBioNet - Task Force COVID-19 Processing and analyzing samples’, sharing the cluster network thus facilitating the downloads. Thanks also to NVIDIA for the generous donation of a Titan Xp and a Quadro P6000.

## Author contributions

These authors contributed equally: Maria de la Iglesia Vayá, Jose Maria Salinas Serrano, Jose Manuel Saborit Torres, Joaquim Angel Montell Serrano, Germán Gonzalez and Aurelia Bustos.

## Competing interests

The authors declare no competing interests.

## References

- [1] ACR. ACR Recommendations for the use of Chest Radiography and Computed Tomography (CT) for Suspected COVID-19 Infection. <https://www.acr.org/Advocacy-and-Economics/ACR-Position-Statements/Recommendations-for-Chest-Radiography-and-CT-for-Suspected-COVID19-Infection>. Accessed: 2020-05-28.
- [2] Jianfang Liu, Tara Lichtenberg, Katherine A Hoadley, Laila M Poisson, Alexander J Lazar, Andrew D Cherniack, Albert J Kovatich, Christopher C Benz, Douglas A Levine, Adrian V Lee, et al. An integrated tcga pan-cancer clinical data resource to drive high-quality survival outcome analytics. *Cell*, 173(2):400–416, 2018.
- [3] Brett K Beaulieu-Jones, Patryk Orzechowski, and Jason H Moore. Mapping patient trajectories using longitudinal extraction and deep learning in the mimic-iii critical care database. In *PSB*, pages 123–132. World Scientific, 2018.
- [4] Alistair EW Johnson, Tom J Pollard, Seth Berkowitz, Nathaniel R Greenbaum, Matthew P Lungren, Chih-ying Deng, Roger G Mark, and Steven Horng. Mimic-cxr: A large publicly available database of labeled chest radiographs. *arXiv preprint arXiv:1901.07042*, 2019.
- [5] Aurelia Bustos, Antonio Pertusa, Jose-Maria Salinas, and Maria de la Iglesia-Vayá. PadChest: A large chest x-ray image dataset with multi-label annotated reports, 2019.
- [6] Joseph Paul Cohen, Paul Morrison, and Lan Dao. COVID-19 Image Data Collection, 2020.

- [7] Jinyu Zhao, Yichen Zhang, Xuehai He, and Pengtao Xie. COVID-CT-Dataset: a CT scan dataset about COVID-19. *arXiv preprint arXiv:2003.13865*, 2020.
- [8] Italian Society of Medical and Interventional Radiology COVID-19 dataset. SIRM. <https://www.sirm.org/category/senza-categoria/covid-19>. Accessed: 2020-05-28.
- [9] Muhammad E. H. Chowdhury, Tawsifur Rahman, Amith Khandakar, Rashid Mazhar, Muhammad Abdul Kadir, Zaid Bin Mahbub, Khondaker Reajul Islam, Muhammad Salman Khan, Atif Iqbal, Nasser Al-Emadi, and Mamun Bin Ibne Reaz. Can AI help in screening Viral and COVID-19 pneumonia?, 2020.
- [10] Lin Li, Lixin Qin, Zeguo Xu, Youbing Yin, Xin Wang, Bin Kong, Junjie Bai, Yi Lu, Zhenghan Fang, Qi Song, et al. Artificial intelligence distinguishes COVID-19 from community acquired pneumonia on chest CT. *Radiology*, page 200905, 2020.
- [11] Shuo Jin, Bo Wang, Haibo Xu, Chuan Luo, Lai Wei, Wei Zhao, Xuexue Hou, Wenshuo Ma, Zhengqing Xu, Zhuozhao Zheng, et al. AI-assisted CT imaging analysis for COVID-19 screening: Building and deploying a medical AI system in four weeks. *medRxiv*, 2020.
- [12] Feng Shi, Liming Xia, Fei Shan, Dijia Wu, Ying Wei, Huan Yuan, Huiting Jiang, Yaozong Gao, He Sui, and Dinggang Shen. Large-scale screening of covid-19 from community acquired pneumonia using infection size-aware classification. *arXiv preprint arXiv:2003.09860*, 2020.
- [13] J. M. S. Serrano, M. A. C. Quevedo, M. de la Iglesia-Vaya, L. Marti-Bonmati, and R. Valenzuela. R and d cloud ceib: Management and knowledge extraction system for bioimaging in the cloud. In *2012 International Conference on Biomedical Engineering and Biotechnology*, pages 469–472, 2012.
- [14] BOE. BOE.es - Documento consolidado BOE-A-2018-16673. <https://www.boe.es/eli/es/lo/2018/12/05/3/con>. Accessed: 2020-05-28.
- [15] Irene Perez-Diez, Raul Perez-Moraga, Adolfo Lopez-Cerdan, Jose-Maria Salinas-Serrano, and Maria de la Iglesia-Vaya. De-identifying Spanish medical texts - Named Entity Recognition applied to radiology reports. *medRxiv*, 2020.
- [16] Kadek YE Aryanto, André Broekema, Matthijs Oudkerk, and Peter MA van Ooijen. Implementation of an anonymisation tool for clinical trials using a clinical trial processor integrated with an existing trial patient data information system. *European radiology*, 22(1):144–151, 2012.

- [17] Jingyi Shi, Jeff Carr, and Yaorong Ge. Development of a flexible imaging data integration tool for multicenter clinical trials. In *Proceedings of the 2nd International Conference on Medical and Health Informatics*, pages 234–237, 2018.
- [18] Jingyi Shi, Jeff Carr, and Yaorong Ge. Development of a Flexible Imaging Data Integration Tool for Multicenter Clinical Trials. In *Proceedings of the 2nd International Conference on Medical and Health Informatics*, ICMHI ’18, page 234–237, New York, NY, USA, 2018. Association for Computing Machinery.
- [19] Mingxing Tan and Quoc V. Le. Efficientnet: Rethinking model scaling for convolutional neural networks, 2019.
- [20] Adam Bernheim, Xueyan Mei, Mingqian Huang, Yang Yang, Zahi Fayad, Ning Zhang, Kaiyue Diao, Bin Lin, Xiqi Zhu, Kunwei Li, Shaolin Li, Hong Shan, Adam Jacobi, and Michael Chung. Chest ct findings in coronavirus disease-19 (covid-19): Relationship to duration of infection. *Radiology*, 295:200463, 02 2020.
- [21] Feng Pan, Tianhe Ye, Peng Sun, Shan Gui, Bo Liang, Lingli Li, Dandan Zheng, Jiazheng Wang, Richard Hesketh, Lian Yang, and Chuansheng Zheng. Time course of lung changes on chest ct during recovery from 2019 novel coronavirus (covid-19) pneumonia. *Radiology*, 295:200370, 02 2020.
- [22] Yuhui Wang, Chengjun Dong, Yue Hu, Chungao Li, Qianqian Ren, Xin Zhang, Heshui Shi, and Min Zhou. Temporal changes of ct findings in 90 patients with covid-19 pneumonia: A longitudinal study. *Radiology*, page 200843, 03 2020.
- [23] Wei Zhao, Zheng Zhong, Xingzhi Xie, Qizhi Yu, and Jun Liu. Relation between chest ct findings and clinical conditions of coronavirus disease (covid-19) pneumonia: A multicenter study. *American Journal of Roentgenology*, 214(5), May 2020.
- [24] Milagros Martí de Gracia, 2020. Available at url=<https://healthcare-in-europe.com/en/news/imaging-the-coronavirus-disease-covid-19.html>.
- [25] OHIF XNAT Viewer, 2020.
- [26] O. Ronneberger, P. Fischer, and T. Brox. U-net: Convolutional networks for biomedical image segmentation. In *Medical Image Computing and Computer-Assisted Intervention (MICCAI)*, volume 9351 of *LNCS*, pages 234–241. Springer, 2015. (available on arXiv:1505.04597 [cs.CV]).
- [27] Krzysztof J. Gorgolewski, Tibor Auer, Vince D. Calhoun, R. Cameron Craddock, Samir Das, Eugene P. Duff, Guillaume Flandin, Satrajit S. Ghosh, Tristan Glatard, Yaroslav O. Halchenko, Daniel A. Handwerker, Michael Hanke, David Keator, Xiangrui Li, Zachary Michael, Camille

Maumet, B. Nolan Nichols, Thomas E. Nichols, John Pellman, Jean-Baptiste Poline, Ariel Rokem, Gunnar Schaefer, Vanessa Sochat, William Triplett, Jessica A. Turner, Gaël Varoquaux, and Russell A. Poldrack. The brain imaging data structure, a format for organizing and describing outputs of neuroimaging experiments. *Scientific Data*, 3(1):160044, 2016.